Hybrid high-order (HHO) method for modeling and numerical simulation of seismic-acoustic wave propagation

Author : Romain Mottier[§†‡] (PhD student) **Supervision** : Alexandre Ern [†‡], Laurent Guillot[§]

[§] French Alternative Energies and Atomic Energy Commission (CEA)
[†] Teaching and Research Center in Mathematics and Scientific Computing (CERMICS)
[‡] French Institute for Research in Numerical Science and Technology (INRIA - SERENA TEAM)

Context and issues

Objectives

- Accurate modelisation and simulation of seismo-acoustic waves **through heterogeneous domains with complex geometries**
- Treatment of realistic cases of interest
  - ▸ **High Performance Computing (HPC)**

Issues

- Difficulty to mesh complex geometries
- High-order precision needed to accurately capture waves
  - ▸ **Hybrid discontinuous methods (HDG/HHO)**

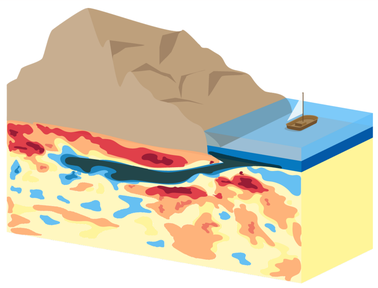

Fig. 1: Lateral heterogeneities near the earth's surface.

Coupling of the acoustic and elastic wave equations

- **Elastic wave equation:**
$$\begin{cases} \partial_t \boldsymbol{\varepsilon}(t) - \nabla^s \boldsymbol{v}^{\mathrm{S}}(t) = \mathbf{0} \\ \rho_{\mathrm{S}} \partial_t \boldsymbol{v}^{\mathrm{S}}(t) - \nabla \cdot (\boldsymbol{\mathcal{C}} : \boldsymbol{\varepsilon}(t)) = \boldsymbol{f}(t) \end{cases}$$
- **Acoustic wave equation:**
$$\begin{cases} \frac{1}{\kappa} \partial_t p(t) + \nabla \cdot \boldsymbol{v}^{\mathrm{F}}(t) = g \\ \rho_{\mathrm{F}} \partial_t \boldsymbol{v}^{\mathrm{F}}(t) + \nabla p(t) = \mathbf{0} \end{cases}$$
- **Coupling condition:**
$$\begin{cases} [\![\boldsymbol{v}(t) \cdot \boldsymbol{n}_\Gamma]\!]_\Gamma = 0 \\ (\boldsymbol{\mathcal{C}} : \boldsymbol{\varepsilon}(t)) \cdot \boldsymbol{n}_\Gamma = p(t) \boldsymbol{n}_\Gamma \end{cases}$$

The HHO method

Degrees of freedom

- **Principle:** Polynomial unknowns located in the cells and on the faces

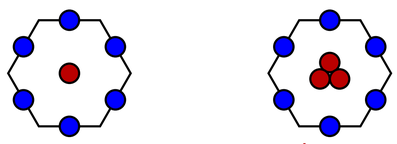

HHO unknowns:
$\hat{u}_h := (u_{\mathcal{T}}, u_{\mathcal{F}})$

Cell unknowns of degree k' **Face unknowns of degree k**

Fig. 2: Left panel: Equal-order discretization ($k' = k = 0$). Right panel: Mixed-order discretization ($k' = k + 1 = 1$).

Operators

- **Gradient reconstruction operator:** $\boldsymbol{\nabla} u \rightarrow \mathrm{G}(\hat{u}_h)$
- **Stabilization operator:** $\mathrm{s}(\hat{u}_h, \hat{w}_h)$
  - ▸ Penalization at the element level to ensure stability while preserving the approximation properties of the reconstruction.

Advantages

- **Mesh flexibility:**
  - ▸ Complex geometries
  - ▸ Unstructured and polyhedral meshes
  - ▸ Local mesh refinement
- **Local conservativity**
- **Optimal error estimates for smooth solutions**
- **Attractive computational costs:**
  - ▸ Global problem couples only face dofs
  - ▸ Cell dofs recovered by local post-processing

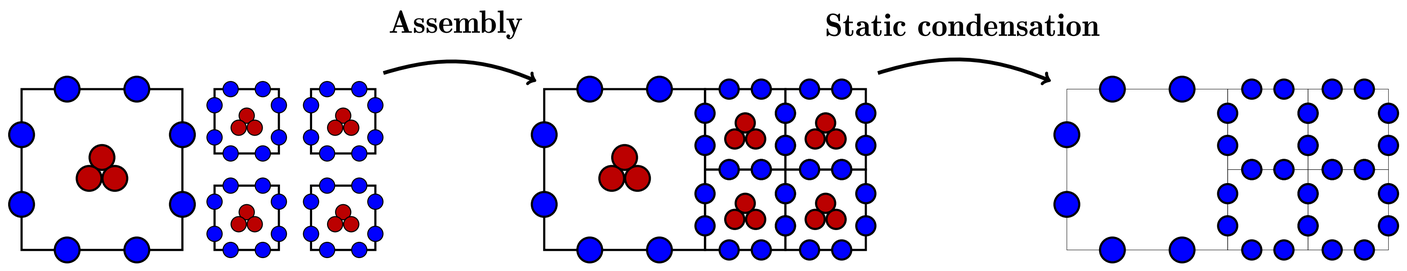

Fig. 3: Static condensation procedure.

HHO space semi-discretization

- **Approximation spaces:**
  - ▸ **Fluid domain:**
$$\boldsymbol{V}_{\mathcal{T}_h^{\mathrm{F}}}^k := \bigtimes_{T \in \mathcal{T}_h^{\mathrm{F}}} \mathbb{P}^k\left(T; \mathbb{R}^d\right), \qquad \hat{V}_h^{\mathrm{F}} := \bigtimes_{T \in \mathcal{T}_h^F} \mathbb{P}^{k'}(T; \mathbb{R}) \times \bigtimes_{F \in \mathcal{F}_h^{\mathrm{F}}} \mathbb{P}^k(F; \mathbb{R})$$
  - ▸ **Elastic domain:**
$$\boldsymbol{\mathcal{Z}}_{\mathcal{T}_h^{\mathrm{S}}}^k := \bigtimes_{T \in \mathcal{T}_h^{\mathrm{S}}} \mathbb{P}^k\left(T; \mathbb{R}^{d \times d}_{\mathrm{sym}}\right), \quad \hat{\boldsymbol{V}}_h^{\mathrm{S}} := \bigtimes_{T \in \mathcal{T}_h^{\mathrm{S}}} \mathbb{P}^{k'}\left(T; \mathbb{R}^d\right) \times \bigtimes_{F \in \mathcal{F}_h^{\mathrm{S}}} \mathbb{P}^k\left(F; \mathbb{R}^d\right)$$

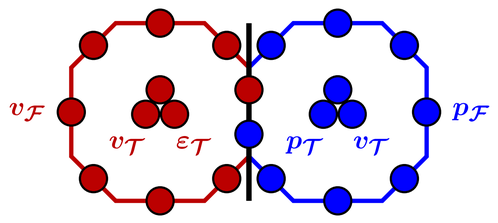

Fig. 4: Elasto-acoustic unknowns with a mixed-order ($k' = k + 1 = 1$) discretization.

- **Elasto-acoustic coupling:**
$$\begin{cases} (\partial_t \boldsymbol{v}_{\mathcal{T}}^{\mathrm{F}}(t), \boldsymbol{r}_{\mathcal{T}})_{\boldsymbol{L}^2(\rho_{\mathrm{F}};\Omega_{\mathrm{F}})} + (\boldsymbol{G}_{\mathcal{T}}(\hat{p}_h(t)), \boldsymbol{r}_{\mathcal{T}})_{\boldsymbol{L}^2(\Omega_{\mathrm{F}})} = 0 \\ (\partial_t p_{\mathcal{T}}(t), q_{\mathcal{T}})_{L^2(\frac{1}{\kappa};\Omega_{\mathrm{F}})} - (\boldsymbol{v}_{\mathcal{T}}^{\mathrm{F}}(t), \boldsymbol{G}_{\mathcal{T}}(\hat{q}_h))_{\boldsymbol{L}^2(\Omega_{\mathrm{F}})} + s_h^{\mathrm{F}}(\hat{p}_h(t), \hat{q}_h) - (\boldsymbol{v}_{\mathcal{F}}^{\mathrm{S}}(t) \cdot \boldsymbol{n}_\Gamma, q_{\mathcal{F}})_{L^2(\Gamma)} = (g(t), q_{\mathcal{T}})_{L^2(\Omega_{\mathrm{F}})} \\ (\partial_t \boldsymbol{\varepsilon}_{\mathcal{T}}(t), \boldsymbol{z}_{\mathcal{T}})_{\boldsymbol{L}^2(\Omega_{\mathrm{S}})} - (\boldsymbol{E}_{\mathcal{T}}(\hat{\boldsymbol{v}}_h(t)), \boldsymbol{z}_{\mathcal{T}})_{\boldsymbol{L}^2(\Omega_{\mathrm{S}})} = 0 \\ (\partial_t \boldsymbol{v}_{\mathcal{T}}(t), \boldsymbol{w}_{\mathcal{T}})_{\boldsymbol{L}^2(\rho;\Omega_{\mathrm{S}})} + (\boldsymbol{\varepsilon}_{\mathcal{T}}, \boldsymbol{E}_{\mathcal{T}}(\hat{\boldsymbol{w}}_h))_{\boldsymbol{L}^2(\mathcal{C};\Omega_{\mathrm{S}})} + s_h^{\mathrm{S}}(\hat{\boldsymbol{v}}_h^{\mathrm{S}}(t), \hat{\boldsymbol{w}}_h) + (p_{\mathcal{F}}(t), \boldsymbol{w}_{\mathcal{F}} \cdot \boldsymbol{n}_\Gamma)_{L^2(\Gamma)} = (\boldsymbol{f}(t), \boldsymbol{w}_{\mathcal{T}})_{\boldsymbol{L}^2(\Omega_{\mathrm{S}})} \end{cases}$$
- **Algebraic realization:**
$$\begin{bmatrix} \mathrm{M}^{\mathrm{v}}_{\mathcal{T}\mathcal{T}} & 0 & 0 & 0 & 0 & 0 \\ 0 & \mathrm{M}^{\mathrm{F}}_{\mathcal{T}\mathcal{T}} & 0 & 0 & 0 & 0 \\ 0 & 0 & 0 & 0 & 0 & 0 \\ 0 & 0 & 0 & \mathrm{M}^{\boldsymbol{\varepsilon}}_{\mathcal{T}\mathcal{T}} & 0 & 0 \\ 0 & 0 & 0 & 0 & \mathrm{M}^{\mathrm{S}}_{\mathcal{T}\mathcal{T}} & 0 \\ 0 & 0 & 0 & 0 & 0 & 0 \end{bmatrix} \begin{bmatrix} \partial_t \mathrm{V}^{\mathrm{F}}_{\mathcal{T}} \\ \partial_t \mathrm{P}_{\mathcal{T}} \\ \partial_t \mathrm{P}_{\mathcal{F}} \\ \partial_t \mathrm{S}_{\mathcal{T}} \\ \partial_t \mathrm{V}_{\mathcal{T}} \\ \partial_t \mathrm{V}_{\mathcal{F}} \end{bmatrix} + \begin{bmatrix} 0 & -\mathrm{G}_{\mathcal{T}} & -\mathrm{G}_{\mathcal{F}} & 0 & 0 & 0 \\ \mathrm{G}^\dagger_{\mathcal{T}} & \Sigma^{\mathrm{F}}_{\mathcal{T}\mathcal{T}} & \Sigma^{\mathrm{F}}_{\mathcal{T}\mathcal{F}} & 0 & 0 & 0 \\ \mathrm{G}^{\mathcal{F}}_{\mathcal{F}} & \Sigma^{\mathrm{F}}_{\mathcal{F}\mathcal{T}} & \Sigma^{\mathrm{F}}_{\mathcal{F}\mathcal{F}} & 0 & 0 & \mathrm{C}_\Gamma \\ 0 & 0 & 0 & 0 & -\mathrm{E}_{\mathcal{T}} & -\mathrm{E}_{\mathcal{F}} \\ 0 & 0 & 0 & \mathrm{E}^\dagger_{\mathcal{T}} & \Sigma^{\mathrm{S}}_{\mathcal{T}\mathcal{T}} & \Sigma^{\mathrm{S}}_{\mathcal{T}\mathcal{F}} \\ 0 & 0 & -\mathrm{C}^\dagger_\Gamma & \mathrm{E}^\dagger_{\mathcal{F}} & \Sigma^{\mathrm{S}}_{\mathcal{F}\mathcal{T}} & \Sigma^{\mathrm{S}}_{\mathcal{F}\mathcal{F}} \end{bmatrix} \begin{bmatrix} \mathrm{V}^{\mathrm{F}}_{\mathcal{T}} \\ \mathrm{P}_{\mathcal{T}} \\ \mathrm{P}_{\mathcal{F}} \\ \mathrm{S}_{\mathcal{T}} \\ \mathrm{V}^{\mathrm{S}}_{\mathcal{T}} \\ \mathrm{V}^{\mathrm{S}}_{\mathcal{F}} \end{bmatrix} = \begin{bmatrix} 0 \\ \mathrm{G}_{\mathcal{T}} \\ 0 \\ 0 \\ \mathrm{F}_{\mathcal{T}} \\ 0 \end{bmatrix}$$

Numerical results

- **Verification of convergence rates on analytical solutions:**
  - ▸ $\mathcal{O}(h^{k+1})$ in H^1-norm ▸ $\mathcal{O}(h^{k+2})$ in L^2-norm **(superconvergence)**

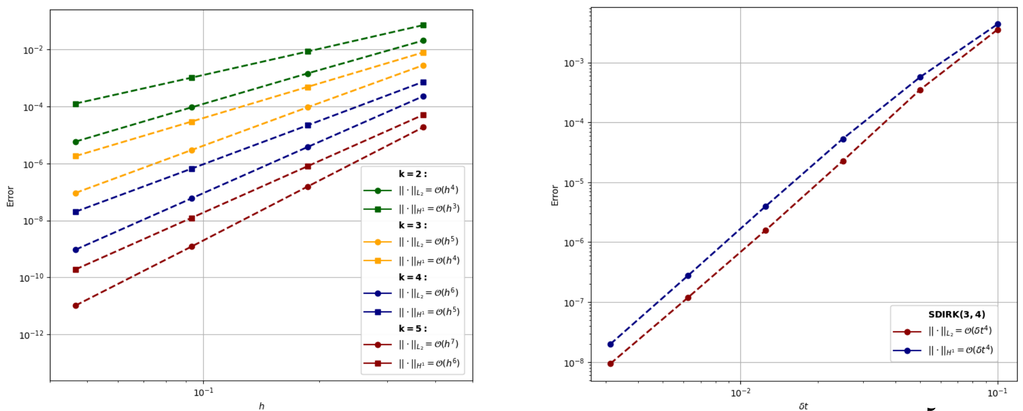

Fig. 5: Left panel: Errors as a function of the mesh size with $\Delta t = 0.1 \times 2^{-5}$. Right panel: Errors as a function of the time-step with $k' = k + 1 = 6$ and $\mathrm{d}x = 2^{-5}$.

- **Realistic test case**
  - ▸ **Computational domain:**
    - Acoustic region on the upper side
    - Elastic region on the lower side
  - ▸ **Homogeneous Dirichlet conditions**
  - ▸ **Intial condition:** pressure Ricker wavelet
$$p_0(x, y) := -\frac{4}{10}\sqrt{\frac{10}{3}}(1600r^2 - 1)\pi^{-1/4}\, e^{-800r^2}$$
$$\boldsymbol{v}_0^{\mathrm{F}} := \mathbf{0}, \qquad \boldsymbol{v}_0^{\mathrm{S}} := \mathbf{0}, \qquad \boldsymbol{\varepsilon}_0 := \mathbf{0}.$$
  - ▸ **Time integration scheme:** SDIRK(s,s+1)

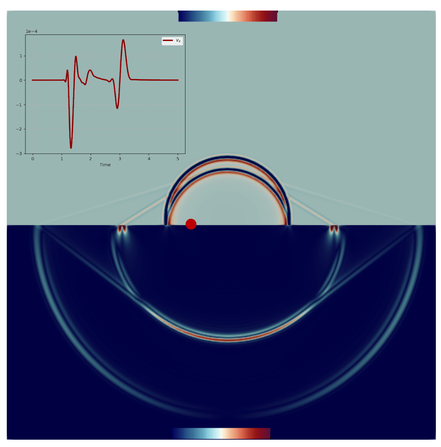

Fig. 6: Two-dimensional distribution of the acoustic pressure (upper side) and elastic velocity norm (lower side), predicted by the HHO-SDIRK $(3, 4)$ at $t = 5$ s. Simulation parameters: $k' = k + 1 = 2, \mathrm{d}x = 2^{-8}$ and $\Delta t = 0.1 \times 2^{-8}$.

Energy conservation of the scheme

- **Mechanical energy of the scheme:** $\mathcal{E}_h(t) := \mathcal{E}_h^{\mathrm{S}}(t) + \mathcal{E}_h^{\mathrm{F}}(t)$ with
$$\mathcal{E}_h^{\mathrm{F}}(t) := \frac{1}{2}||\boldsymbol{v}_{\mathcal{T}}^{\mathbf{F}}(t)||^2_{\boldsymbol{L}^2(\rho_{\mathrm{F}};\Omega_{\mathrm{F}})} + \frac{1}{2}||p_{\mathcal{T}}(t)||^2_{L^2(\frac{1}{\kappa};\Omega_{\mathrm{F}})}, \qquad \mathcal{E}_h^{\mathbf{S}}(t) := \frac{1}{2}||\boldsymbol{v}_{\mathcal{T}}^{\mathbf{S}}(t)||^2_{\boldsymbol{L}^2(\rho_{\mathrm{S}};\Omega_{\mathrm{S}})} + \frac{1}{2}||\boldsymbol{\varepsilon}_{\mathcal{T}}(t)||^2_{\boldsymbol{L}^2(\mathcal{C};\Omega_{\mathrm{S}})}$$
- **Semi-discrete energy conservation of the scheme**
$$\mathcal{E}_h(t) = \mathcal{E}_h(0) + \int_0^t \left[(\boldsymbol{f}(\alpha), \boldsymbol{v}_{\mathcal{T}}^{\mathrm{S}}(\alpha))_{\boldsymbol{L}^2(\Omega_{\mathrm{S}})} + (g(\alpha), p_{\mathcal{T}}(\alpha))_{L^2(\Omega_{\mathrm{F}})} - s_h^{\mathrm{S}}(\hat{\boldsymbol{v}}_h^{\mathrm{S}}(\alpha), \hat{\boldsymbol{v}}_h^{\mathrm{S}}(\alpha)) - s_h^{\mathrm{F}}(\hat{p}_h(\alpha), \hat{p}_h(\alpha)) \right] \mathrm{d}\alpha$$
- **Validation on analytic test cases**

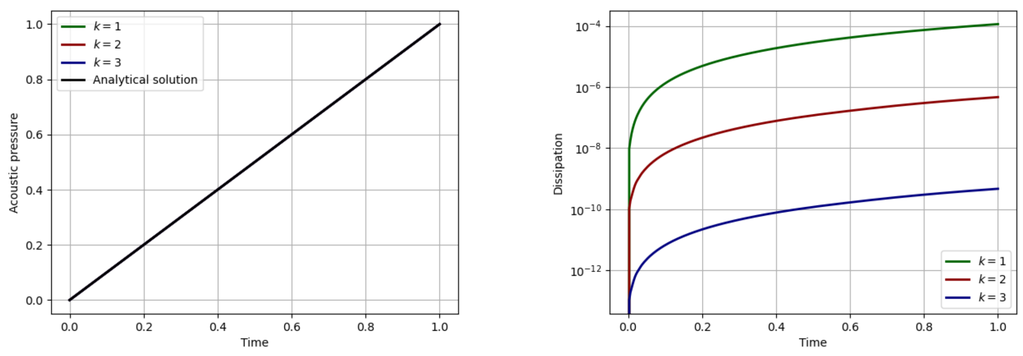

Fig. 7: Demonstration of the negligible nature of the energy dissipation introduced by the HHO scheme.

Some references

[1] Di Pietro and Ern. "A hybrid high-order locking-free method for linear elasticity on general meshes". In: *Comput. Meth. Appl. Mech. Engrg.* 283 (2015), pp. 1–21.

[2] Burman, Duran, and Ern. "Hybrid high-order methods for the acoustic wave equation in the time domain". In: *Comm. App. Math. Comp. Sci.* 4.2 (2022), pp. 597–633.

[3] Burman, Duran, Ern, and Steins. "Convergence Analysis of Hybrid High-Order Methods for the Wave Equation". In: *J. Sci. Comput.* 87.3 (2021), p. 91.

[4] Terrana, Vilotte, and Guillot. "A spectral hybridizable discontinuous Galerkin method for elastic-acoustic wave propagation". In: *Geophys. J. Int.* 213.1 (2017), pp. 574–602.